

# Universality, the BNN relation, and scaling for dispersive ionic materials

*J. Ross Macdonald*

*Department of Physics and Astronomy, University of North Carolina,*

*Chapel Hill, NC 27599-3255, USA; Tel.: +1-919-967-5005; [macd@email.unc.edu](mailto:macd@email.unc.edu)*

Many frequency-response analyses of experimental-data for homogeneous glasses and single-crystals indicate that estimates of the stretched-exponential  $\beta_1$  shape parameter of the K1 fitting model are close to 1/3 and are virtually independent of both temperature and ionic concentration. This model, which yields better fits than others, is indirectly associated with temporal-domain stretched-exponential response having the same  $\beta_1$  parameter value. Here it is shown that hopping theory yields the important and unique value of 1/3 for the  $\beta_1$  of the K1 model. It is therefore appropriate to fix the  $\beta_1$  parameter of this model at a constant value of 1/3, defined as the U model. It fits data sets that vary with both temperature and concentration just as well as those with  $\beta_1$  free to vary, and it leads to a correspondingly universal value of the Barton-Nakajima-Namikawa (BNN) parameter  $p$  of 1.65. U-model complex-nonlinear-least-squares data fitting, taking account of the bulk dipolar-electronic dielectric constant,  $\epsilon_{D\infty}$ , and of electrode effects when significant, also leads to two hopping-parameter estimates that yield optimum scaling of such composite experimental data involving both temperature and concentration variation, demonstrated here for data in complex-resistivity-plane form, and for data transformed to the  $M''$  and  $\sigma'$  immittance levels.

PACS numbers: 66.30.Dn, 61.47.Fs, 77.22.Gm, 72.20.-i, 66.10.Ed.

## I. INTRODUCTION

In 1994 Phillips suggested that the most important unsolved problem in physics today is to explain relaxation in complex (disordered) systems by microscopic analysis [1]. Roling and Martiny have recently stated that “Finding an explanation for this high degree of universality (i.e., the existence of master-curves for conductivity isotherms) is still one of the major challenges of solid state physics” [2]. The present work addresses both these challenges. The apparent universality of conduction in disordered solids has been discussed by Dyre and Schröder who suggested various macroscopic and microscopic models that predict such universality in the extreme disorder limit [3]. Since universality is an idealized concept, it is not surprising that most claims for universal behavior and models [e.g., 4,5] have been found too limited or even incorrect, but this should not discourage new universality proposals, ones that are generally doomed eventually to suffer the same fate as new experimental results are analyzed and the domain to which the model is applied is sufficiently extended.

It has been found that for conduction involving charge carriers of a single type in many different materials, including homogeneous glasses and even single crystals, the K1 response model, discussed below and indirectly derived from stretched-exponential temporal response, yields excellent complex-nonlinear-least-squares (CNLS) fits of experimental frequency response data with a free shape parameter  $\beta_1 \approx 1/3$  [6-9]. Such fits are generally superior to those using other models, and in fact, the K1 model with  $\beta_1$  fixed at  $1/3$ , yields results equivalent to or often somewhat better than those with it taken free to vary. The result of this choice will be termed the U model, thus underlining its wide applicability. Fitting of dispersive data involving hopping charge carriers with a model such as the U one leads to parameter estimates that yield important

information about charge transport in the material considered. Further, it provides optimum values of quantities that may be used for scaling data under variation of temperature and charge concentration.

The U model involves only the free parameters  $\rho_0 \equiv 1/\sigma_0$  and  $\tau_o$ , ones that determine scale and position on the frequency axis, respectively. Here  $\rho_0$  is the dc resistivity and  $\tau_o$  is the characteristic relaxation time of the K1 model. Since the  $\beta_1 = 1/3$  value is found experimentally to be virtually independent of both temperature and ionic concentration, the shape of U-model response is likewise independent of these variables, yielding a high degree of universality. Because of the influence of a bulk high-frequency-limiting dielectric constant,  $\epsilon_{D\infty}$ , associated with dipolar and vibratory effects, on all frequency-responses except those of  $\sigma'(\omega)$  and  $\epsilon''(\omega)$ , the part of the U model that describes conductive-system hopping response alone must be augmented by the inclusion of an additional free parameter,  $\epsilon_x$ , to represent  $\epsilon_{D\infty}$  except when fitting the above two responses. Further, it is often found necessary to include a series constant-phase element or even a more complicated series response combination in order to take account of electrode blocking and polarization effects present in typical frequency-response data [7,10]. When such a composite model yields excellent fitting of the total data, those parameters associated only with the dispersive response of the material, such as  $\rho_0$ ,  $\tau_o$ , and  $\beta_1$ , are optimally estimated and separated from other non-dispersive processes that may influence the data. There has been very little such fitting carried out by others in the past, so it is important to demonstrate its utility and power.

## II. DETAILS OF CONDUCTIVE-SYSTEM DISPERSIVE MODELS

Let the index  $k$  take on values of 0 and 1, eventually designating the K0 and K1 conductive-system response models. Then if  $\phi_0(t)$  is a correlation function defined in the time domain, the corresponding normalized frequency response complex function, defined at the complex resistivity level, is [ 9,11]

$$I_0(\omega) = I_0'(\omega) - iI_0''(\omega) = \frac{\rho_{C0}(\omega) - \rho_{C0}(\infty)}{\rho_{C0}(0) - \rho_{C0}(\infty)} = \int_0^\infty \exp(-i\omega t) \left( -\frac{d\phi_0(t)}{dt} \right) dt \quad (1)$$

When the small or zero  $\rho_{C0\infty} \equiv \rho_{C0}(\infty)$  quantity is neglected [12], the corresponding  $k=0$  frequency response at the complex modulus level is  $M_{C0}(\omega) = i\omega\varepsilon_V\rho_0 I_0(\omega)$ . Here the subscript ‘‘C’’ denotes conductive-system response and  $\varepsilon_V$  is the permittivity of vacuum. We shall not distinguish between  $\rho_{C0}(0)$ ,  $\rho_{C1}(0)$ , and  $\rho_0$ .

When the famous 1973 continuous-time, random-walk (CTRW) approximate microscopic model of Scher and Lax [13] is extended slightly to make its imaginary part fully consistent with its real part at the complex conductivity level [12], this conductive-system model may be expressed at the complex modulus level as [9,12]

$$M_{C1}(\omega) = M_{C1}'(\omega) + iM_{C1}''(\omega) = i\omega\varepsilon_V\rho_0 I_1(\omega) \equiv [1 - I_{01}(\omega)] / \varepsilon_Z, \quad (2)$$

where  $\varepsilon_Z = \varepsilon_{C1}'(\infty) \equiv \varepsilon_{C1\infty} = 1 / M_{C1}(\infty)$ , and the 01 subscript indicates that  $I_{01}(\omega)$  is just  $I_0(\omega)$  in form but it involves the  $I_1(\omega)$  shape-parameter fitting estimate rather than the value that would be obtained by direct fitting with the  $k=0$  model involving  $I_0(\omega)$ . In Ref. 13, the  $\phi_0(t)$  correlation function that leads to  $I_0(\omega)$  normalized frequency response is defined as the probability that a hopping entity remains fixed in place over the time interval from 0 to  $t$ .

Equation (2) provides a direct connection between the different  $I_1(\omega)$  and  $I_0(\omega)$  responses, but the time domain response following from  $I_1(\omega)$  is not the same as that of  $I_0(\omega)$  [12]. Importantly, Eq. (2), arising from a microscopic analysis, is of exactly the same form as that derived macroscopically and contemporaneously by Moynihan, Boesch, and Laberge [14] by considering electric field decay at constant dielectric displacement, thus providing consistency and further justification for this model. It remains general, however, until specific forms of  $\phi_0(t)$  and  $\varepsilon_Z$  are introduced.

It follows from the work of Scher and Lax, Eq. (2), and Refs. [6,9,12, and 15] that for the general dispersion model,  $\varepsilon_Z = \varepsilon_{C1\infty}$  may be expressed as

$$\varepsilon_{C1\infty} = (\sigma_0 / \varepsilon_V) / \langle \tau^{-1} \rangle_1 = \varepsilon_{Ma} \langle x \rangle_{01} = [\gamma N (qd)^2 / (6k_B \varepsilon_V)] / T. \quad (3)$$

Here  $x \equiv \tau / \tau_o$ ;  $\varepsilon_{Ma} \equiv \sigma_0 \tau_o / \varepsilon_V$ ; and  $\langle \tau^{-1} \rangle_1$  and  $\langle \tau \rangle_{01} \equiv \tau_o \langle x \rangle_{01}$  are different averages over the  $k=1$  and  $k=0$  distributions of relaxation times, ones determined by the choice of  $\phi_0(t)$ . In addition,  $N$  is the maximum mobile charge number density;  $\gamma$  is the fraction of charge carriers of charge  $q$  that are mobile; and  $d$  is the rms single-hop distance for the hopping entity. The high-frequency-limiting effective dielectric constant,  $\varepsilon_{C1\infty}$ , associated entirely with mobile-charge effects, is likely to arise from the short-range vibrational and librational motion of caged ions. Equation (3) is consistent with the Scher-Lax result that  $\rho_0$  is proportional to  $\langle \tau \rangle_{01}$ , identified in their work as the mean waiting time for a typical hop [12,13,15].

### A. Specific models associated with stretched-exponential temporal response

The ubiquitous stretched-exponential relation,  $\phi_0(t) = \exp\{-(t/\tau_o)^{\beta_0}\}$  with  $0 < \beta_0 \leq 1$  [16,17], originally introduced by Kohlrausch, was used in Eq. (1) to obtain an explicit expression

for the modulus-level frequency response of Eq. (2) [14] and thereby yields both the K0 and K1-model responses [9], ones that must be calculated numerically. The free LEVM CNLS computer program allows these responses to be very accurately determined, however, for both fitting and simulation tasks [18]. When the form of  $\phi_0(t)$  is known, one can calculate  $\langle \tau \rangle_0$  from

$$\langle \tau \rangle_0 = \int_0^{\infty} \phi_0(t) dt \quad [11,13].$$

The pioneering treatment of Ref. [14], now termed the original modulus formalism approach and involving the  $k=1$  K1 response model, is unfortunately critically flawed by the identification of  $\varepsilon_z$  as  $\varepsilon_{\infty} \equiv \varepsilon'(\infty)$ , a quantity that includes all contributions to the high-frequency-limiting dielectric constant. Since the authors did not recognize the existence of  $\varepsilon_{C1\infty}$ , their  $\varepsilon_{\infty}$  was considered to be just  $\varepsilon_{D\infty}$ , rather than  $\varepsilon_{\infty} = \varepsilon_{C1\infty} + \varepsilon_{D\infty}$ . In the usual case where both quantities are non-zero, data fitting would yield an estimate of  $\varepsilon_{\infty}$ , identified as  $\varepsilon_{D\infty}$ , but actually including both contributions [7,9]. The failure to distinguish between these two quantities led to an implicit mixing of dipolar dielectric effects and those associated only with mobile charge and thus to both theoretical and experimental inconsistencies [7,9,19]. Fitting of  $M''(\omega)$  data using the original modulus formalism and the K1 model has, since 1973, yielded strong dependence of the estimated  $\beta_1$  values on ionic concentration and appreciable temperature dependence as well, but these results must be fully discounted.

In contrast, the corrected modulus formalism also uses the K1 model but treats  $\varepsilon_{D\infty}$  separately, leading to virtually constant estimates of  $\beta_1$  along with both better fitting and no inconsistencies [19]. For the K1 with  $\varepsilon_z = \varepsilon_{C1\infty}$  in Eq. (2), Eq. (3) may be expressed as

$$\varepsilon_{C1\infty} = \varepsilon_{Ma} \langle x \rangle_{01} = \varepsilon_{Ma} \beta_{1C}^{-1} \Gamma(\beta_{1C}^{-1}) = A/T, \quad (4)$$

where  $A$  is the term in square brackets at the right-side end of Eq. (3) and depends on ionic concentration but not appreciably on temperature [7];  $\Gamma(\cdot)$  is the Euler gamma function; and  $\beta_{1C}$  is a value of  $\beta_1$  obtained from fitting using the corrected modulus formalism with a separate free parameter to estimate  $\varepsilon_{D\infty}$ . It follows from Eq. (4) that when  $A$  is temperature independent, the thermally activated quantities  $T\sigma_0$  and  $\tau_o$  each exhibit Arrhenius behaviour and their product is itself temperature independent.

### B. The U model and some of its consequences

Now when one sets  $\beta_{1C}$  fixed at  $1/3$  in the K1 model of Eqs. (2) and (4) to obtain the U response model, one finds that  $\varepsilon_{C1\infty} = 6\varepsilon_{Ma}$ ,  $\varepsilon_{C10} \equiv \varepsilon_{C1}'(0) = 60\varepsilon_{Ma}$ , and so  $\Delta\varepsilon_{C1} \equiv \varepsilon_{C10} - \varepsilon_{C1\infty} = 54\varepsilon_{Ma} = \Delta\varepsilon$ , since  $\varepsilon_{D\infty}$  subtracts out, one of the virtues of using  $\Delta\varepsilon$  rather than either of its two components. In addition, if one defines  $\varepsilon_{C1S}''(\omega) \equiv \varepsilon_{C1}''(\omega) - (\sigma_0/\omega\varepsilon_V)$ , then the resulting dielectric loss involves a peak response at  $\nu_p \equiv \omega_p/2\pi \cong 0.01122/2\pi\tau_o$ , with  $\varepsilon_{C1S}''(\omega_p) \cong 14.405\varepsilon_{Ma}$  for the peak value.

An expression that has been of considerable importance in the past is that of Barton [20], Nakjima [21], and Namikawa [22], commonly known as the BNN relation,

$$\sigma_0 = p\varepsilon_V\Delta\varepsilon\omega_p, \quad (5)$$

where  $p$  is numerical constant of order 1, and  $\omega_p$  is the dielectric loss peak, only equal to the value listed above for the U model. For that model, however, it follows that  $p = 1/(0.01122 \times 54) \cong 1.65$ , a universal value for all data that are well fitted by the U model.

Figure 3 in Ref. 3 is a log-log BNN-related plot that indicates that most estimates of  $p$  are close to the above value, a satisfying result in view of the usual uncertainties associated with estimates of  $\Delta\varepsilon$  and  $\omega_p$  from experimental data. Although Porto *et al.* [23] have recently questioned the applicability of the BNN relation for changes in charge carrier concentration, excellent U-model fittings for wide variation in concentrations, Ref. 7 and the results discussed below, show that estimates of  $p$  from such fits confirm the 1.65 value. Thus, it will usually be appropriate in future to replace the BNN relation by any of those listed above that connect effective dielectric quantities, such as  $\varepsilon_{C1\infty}$ , to the Maxwell quantity  $\varepsilon_{Ma}$ .

### C. Physical interpretations of the U-model $\beta_1 = 1/3$ value

Since the macroscopic/microscopic U-model leads to superior fits of the frequency response of all single-ion materials investigated so far, a plausible physical interpretation of its  $\beta_{1C} = \beta_{01} = 1/3$  value is needed. Much work in the field of dispersive conductive systems, especially that using the original modulus formalism approach, has taken the stretched-exponential  $\beta$  as just a fitting parameter or has interpreted it as a measure of correlation between hopping ions. But both the inapplicability of the original modulus formalism approach and corrected modulus formalism fit results involving a constant value of  $\beta_{1C} \cong 1/3$  require rejection of this physical interpretation.

Although Phillips [1,24] has treated stretched exponential relaxation in great detail, this work was primarily limited to consideration of mechanical and dielectric relaxation results for non-conductors, with little consideration of  $\beta_1$  estimates obtained from data involving frequency

dispersion associated with mobile charge carriers. As he discusses, however, several treatments of the trapping model involving fixed trapping sites lead to the result

$$\beta = d_e / (2 + d_e), \quad (6)$$

where  $d_e$  is the effective dimensionality of the configuration space in which dispersive effects occur.

For Coulomb interaction, the value  $d_e = 3/2$  was derived, leading to  $\beta = 4/7$ , while for spin glasses on cubic lattices a value of  $1/3$  was obtained with  $d_e = 1$ . The spin-glass model is not directly appropriate for the present situation, and the maximum-disorder universal-model treatments of Dyre and Schrøder [3] do not involve explicit Coulomb effects. A value of  $d_e = 1.35$  was found to be most appropriate by these authors. Further, there is no reason to believe that the stretched exponential waiting-time distribution,  $\phi_0(t)$  with  $0 < \beta_0 \leq 1$ , necessarily includes such effects.

The U model involves the value  $\beta_{01} = 1/3$ , implying a value of  $d_e = 1$  when Eq. (6) is applicable. But the corrected modulus formalism using the K1 model determines the value of  $\beta_{1C}$  from fitting experimental data, and thus directly determines the above value of  $\beta_{01}$ , one that does not follow from K0 fitting of the same data. In fact, the high-frequency-limiting log-log slope of  $\sigma'(\omega)$  for the U model is  $1 - \beta_{1C} = 2/3$ . Similarly, the corresponding high-frequency limiting slope of  $\sigma'(\omega)$  for the corresponding K0 model with  $\beta_0$  fixed at  $2/3$  is also  $2/3$ , so  $\beta_0 = 1 - \beta_{1C}$  in the limit. Nonlinear least squares K0-model fitting of limited-range U-model  $\sigma'(\omega)$  data leads to a maximum 15% difference in the initial curved region of the  $\sigma'(\omega)$  response and to  $\beta_0$  estimates

that generally fall in the range from 0.5 to  $2/3$  as the range of the data is increased to include larger and larger values of  $\sigma'(\omega)$ .

Some implications of the above results are as follows. The Scher-Lax stochastic model [13] is a 3D one that treats all sites on a discrete lattice as equivalent and independent and leads to frequency response substantially different from that of a later on-off one-dimensional bond-percolation stochastic model [25,26]. Thus, the  $\beta_{1c} = \beta_{01} = 1/3$  value need not directly imply that the motion of the hopping charge carriers is one dimensional but it certainly indicates that the stretched-exponential correlation function determining the K0 and K1 responses involves a waiting-time distribution best interpreted in terms of physical processes occurring in a configuration space with an effective dimension of unity. In contrast, if Eq. (6) were applied directly to the K0 model, then the  $\beta_0 = 2/3$  value would be associated with an implausible effective dimensionality of 4. These conclusions raise the need for a detailed microscopic treatment that justifies the U-model requirement that the effective dimensionality of its waiting-time distribution be unity.

Although a recent geometric derivation of stretched-exponential response for mobile electrons leads to a continuously variable  $\beta$  [27] and so is not relevant to the present results, a much earlier CTRW treatment [16,17], involving some elements of the Scher-Lax model derivation, showed that the value of  $\beta$  was determined by the rate at which a hopping entity finds a new site, and that if  $\beta(1)$  is that for one-dimensional hopping, then  $\beta(3)$ , that for an effective dimension of 3, equals  $2\beta(1)$ . Thus, if  $\beta(1) = 1/3$ , the theory requires that  $\beta(3) = 2/3$ . But note that  $\beta_0 = 1 - \beta_{1c}$ , and if we identify  $\beta_0$  as  $\beta(3)$  and  $\beta_{1c}$  as  $\beta(1)$ , as indicated by the U-model fitting results, then we may write  $\beta(3) = 1 - \beta(1) = 2\beta(1)$ . Thus the above two relations require not

only that  $\beta(1)=1/3$  but they show that this is the *only* value that is consistent here with  $\beta(3) = 2\beta(1)$ .

These important results are thus consistent not only with the experimental  $\beta_{1c} = 1/3$  fitting result but also with the  $2/3$  limiting-slope value found for K0-model fits and for the 3D Scher-Lax model. The interesting and important question of why data fitting results using the latter discrete-lattice model involving a stretched-exponential correlation factor lead to both the 1D  $\beta_{1c}$  value of  $1/3$  and the 3D slope value of  $2/3$  instead of the  $3/5$   $\beta$  one associated with non-conducting continuum 3D models [1] has been recently justified by an independent physically based topological approach [28], thereby further supporting the appropriateness of the present  $\beta$  values.

### III. FITTING AND SCALING RESULTS FOR THE U MODEL

When one has available an excellent fitting model applicable for a particular experimental and material domain, there is no need for scaling since data fitting with such a model leads to explicit parameter estimates and thus to more information than does development of a master scaling model. Although the U model is thus superior to scaling within its domain of applicability, it is instructive to discuss scaling parameters following from it and to show their applicability for data that include variation of both temperature and ionic concentration. For this purpose, data for the following materials will be used, as listed in Table I:  $0.5\text{Li} \bullet 0.5\text{La} \bullet \text{TiO}_3$ ,  $x_c\text{K}_2\text{O} \bullet (1-x_c)\text{GeO}_2$ , and  $0.3(0.6\text{Na}_2\text{O} \bullet 0.4\text{Li}_2\text{O}) + 0.7\text{B}_2\text{O}_3$ . I thank Drs. León, Jain, and Roling, respectively, for kindly providing these data sets.

### A. Scaling possibilities and limitations

Before presenting fitting and scaling results for these materials, it is desirable to consider scaling approaches. It has been customary to write a general scaling relation in the form

$$\sigma'(\omega)/\sigma_0 \equiv \rho_0 \sigma'(\omega) = F'(\omega\tau_s) \equiv F'(v/v_s), \quad (7)$$

where the left-hand parts refer to data and the right-hand ones to a fitting model, and  $v_s \equiv 1/(2\pi\tau_s)$ . The essence of good scaling then involves choosing appropriate  $v_s$  scaling values. Usually, no fitting is actually carried out, and an equation such as (7) is merely written to define the type of scaling to be used for  $\sigma'(\omega)$  data. Various explicit choices for  $v_s$  and discussions of the historical background of scaling appear in Refs 2, 3, 6, and 23. Here, scaling will be carried out employing a fully complex version of Eq. (7) for fitting, one that may be used to fit complex data at any immittance level and may include non-hopping processes.

Of the many past choices for  $v_s$ , we here consider only those of Sidebottom [5], Dyre and Schrøder [3], Macdonald [6], and Roling and Martiny [2]. The first two are essentially equivalent, are both related to the BNN relation, and when expressed in terms of  $\varepsilon_{Ma}$  are:  $v_s \equiv (\varepsilon_{Ma}/\Delta\varepsilon)\tau_o^{-1}$  and  $v_s \equiv (\varepsilon_{Ma}/\Delta\varepsilon)/(2\pi\tau_o)$ , respectively. For the U model, where  $\tau_s$  becomes the explicit characteristic response time of the model,  $\tau_o$ , estimated from data fitting, these results lead to  $v_s = 0.0185/\tau_o$  and  $v_s = 0.00295/\tau_o$ . In contrast, the earlier work of the author [6] involved just the  $\tau_o$  quantity derived from corrected modulus formalism fits of the K1 model. For the U model, that result becomes  $v_s \equiv 1/(2\pi\tau_o) = 0.1592/\tau_o$ . Finally, Roling and Martiny set  $v_s \equiv v_p$ , where  $v_p$  is the frequency at the peak of the mobile-charge dielectric loss response, discussed in Section II-B. For the U model, the frequency of the  $\varepsilon_{c1s}''(\omega_p)$  peak is  $v_p = 0.001786/\tau_o$ , a factor of exactly the U-model BNN  $p$  value of 1.65 smaller than the Dyre and Schrøder result,

The differences in the numerical values of the numerators of the expressions for all of the above scaling quantities are not significant for scaling, so they are all equivalent in this sense. Nevertheless, the choice of a proper value of  $\tau_o$  is of the greatest importance for good scaling. Note, however, that since  $\Delta\varepsilon$  and  $\nu_p$  may be directly estimated from experimental data without fitting, a good estimate of  $\tau_o$  is not actually necessary to form a scaling value of  $\nu_s$  when a value of  $\sigma_o$  is available, also necessary for scaling of  $\sigma'(\omega)$  itself.

But consider the following: the estimation of  $\Delta\varepsilon$  from data requires separate estimated values of both  $\varepsilon_o$  and  $\varepsilon_\infty$ . Estimation of both of these quantities, especially that of  $\varepsilon_o$ , is rendered uncertain by the usual presence of electrode effects, as demonstrated in the next section; in addition the data often do not extend to high enough frequencies to yield a good estimate of  $\varepsilon_\infty$ . Further, estimation of  $\nu_s \equiv \nu_p$  requires subtraction using a good estimate of  $\sigma_o$  and then the determination of the frequency of the peak of a curve that usually varies very slowly in the neighbourhood of the peak, again an inherently inaccurate process for ordinary experimental data.

## **B. U-model fitting**

The above discussion shows that the usual determination of scaling factors may depend on the use of only one or two points of the data, rendering results uncertain. On the other hand, CNLS estimation of values of  $\sigma_o$ ,  $\tau_o$ , and  $\varepsilon_{C1\infty}$  from U-model fitting makes use of all the data in an optimum way, also provides an estimate of  $\varepsilon_{D\infty}$ , and allows electrode effects to be adequately accounted for as part of the fitting. Therefore, scaling with values of these quantities so estimated is much more appropriate than are other approaches. Let us define the resulting scaled variables as  $\bar{\sigma} \equiv \sigma/\sigma_o$  and  $\bar{\nu} \equiv \omega\tau_o \equiv \bar{\omega} \equiv \nu/\nu_s$ , where  $\nu_s \equiv 1/(2\pi\tau_o)$ .

Fitting results are presented in Table I. All fits of experimental data shown here used the U model with an extra free parameter to estimate  $\varepsilon_{D\infty}$  and usually with additional free parameters (not shown) to account for electrode polarization effects. Other fits of the present data using the K1 model with  $\beta_1$  free to vary led to estimates of it that were, as usual, very close to 1/3. See also the fitting results of Refs. 7 and 28 for results for other materials. Even when the relative standard deviation,  $S_F$ , of one of these fits with  $\beta_1$  free was slightly smaller than that obtained with it fixed at 1/3, the relative standard deviations of the free parameters were smaller than those with it free, indicating a more significant fit. It is also worth emphasizing that comparison of the  $\tau_o$  estimates for the two types of fit show that they are far less stable than those of  $\beta_1$  since a small change in the estimate of the latter results in an appreciable change in the corresponding  $\tau_o$  estimate.

The results shown in the A and B and C and D rows in the table are consistent with earlier work where K1-model fits of the present kind led to  $\beta_1 \cong 1/3$  estimates that were nearly independent of both temperature and ionic concentration, making it reasonable to use the fixed value of  $\beta_1 = 1/3$  in the present work. It is worth noting, however, that the A and B row estimates of  $\varepsilon_{C1\infty}$  are not exactly proportional here to  $1/T$ , as expected from Eq. (4) and from earlier work [7]. Although this discrepancy may be associated with the large role that electrode effects play in the present data, as indicated in the response curves presented below, it is somewhat more likely to be associated with non-Arrhenius behaviour stemming from a physically reasonable low-end cutoff of the K1 distribution of relaxation times.

The U line in the table involves only K1-model response with  $\beta_1$  fixed at a value of 1/3 and the other two parameters each having their scaled values of 1. When, in addition,  $\varepsilon_v$  is also set to the scaled value of 1, then from Eq. (3)  $\bar{\varepsilon}_{C1\infty} = 6$ . All of the K0 results in the table involved real-

part fitting except the listed  $\bar{\varepsilon}_{C1\infty}$  value where full complex-data fitting was used. Such fitting necessarily used both the K0 model and a free dielectric-constant parameter to account for the presence of  $\bar{\varepsilon}_{C1\infty}=6$  in the U-model scaled data. The scaled  $\bar{\sigma}'(\bar{\nu})$  U-model data, designated UM, extended up to a maximum value of  $10^5$ , where the slope was about 0.664, and was fitted to the K0 model using nonlinear least-squares. The last column in the K0 row shows its  $\beta_0$  estimate in square brackets. An appreciably larger frequency range would be needed for the resulting  $\beta_0$  estimate to more closely approximate its limit of  $2/3$ .

Note that although the present K0-model fit of the virtually exact K1 synthetic data leads to a value of  $\bar{\varepsilon}_{C1\infty}$  reasonably close to the exact value of 6, the estimate of  $\bar{\tau}_o$  is about 18 rather than 1. Such a larger value than that for the K1 model is characteristic of K0 fits. Finally, the other quantities in the last column of the table are percentage  $S_F$  values for fits of each set of data after subtracting the effects of estimated  $\varepsilon_{D\infty}$  and electrode polarization parameters from the original data and then fitting the results of such subtraction to the scaled U model. As expected, such subtraction of comparable quantities leads to less accurate fits than those involving the full data but the two parameter estimates of the model were nevertheless very close to the exact U-model data values of unity.

### C. U-model scaling

Complex plane plots of resistivity data are particularly useful in showing electrode effects when present. In order to compare curves for different materials and conditions, all the figures presented here involve data scaled as above using  $\rho_0$  and  $\tau_o$  values estimated from the unscaled U-model fits of Table I. Figure 1 presents such results for the A and B material listed in the table. In

order to maximize clarity, not all points used in fitting are included in this and the other figures. In Figure 1 only about half of the data points are plotted, and, in addition, for the B data the right-hand spur extending to over 1.3 for the actual fitting was cutoff as shown. No such cutoff was applied for the A results.

The figure shows that the original (scaled) data lines for the two temperatures are similar for the high-frequency response region but begin to diverge at the lowest frequencies. The remaining two curves are those for data from which the effects of  $\varepsilon_{D\infty}$  and electrode polarization have been subtracted before scaling, a simple procedure after LEVM fitting. It is clear that in the present representation, the non-hopping contributions dominate hopping ones except at the high-frequency end of the curves. Further, we see that the remaining hopping results fall closely on the U-model master curve solid line, although those for the A situation show a bit more deviation than do the B ones.

It is particularly important to emphasize that, to the degree that the non-hopping effects were adequately estimated by the fit of the full data, the hopping response shown here does not consist of points fitted to the master curve but instead it represents the best *hopping-data* estimates obtained from the fits of the full data. The excellent agreement with the exact U-model master curve of the hopping points for both temperatures shows not only that the present scaling is appropriate but that the hopping response is indeed very well described by the U model and its assumption of  $\beta_1 = 1/3$ . As we shall see, these conclusions are further confirmed by the results shown in the subsequent figures. The use of U-model fitting to allow the non-hopping contributions to the full response to be eliminated does not guarantee that the resulting data points will lie close to the U-model hopping curve. That they actually do so is confirmation that the U model represents the dispersive hopping part of the response adequately.

Figure 2 shows a more stringent fitting situation; one where the unscaled dispersive part of the response is much smaller for the low-concentration D condition than that for the C one. Here, in order to maximize resolution and clarity the y-axis-scale unit length is made greater than the x-axis one; so this is not quite a traditional complex-plane plot. Electrode effects are somewhat less apparent for the present data than are those of Fig. 1, and the differences between the original-data curves and those representing only hopping arise primarily from the relative sizes of the dispersive contributions and those directly associated with the scaled values of  $\rho_0$  and  $\varepsilon_{D\infty}$ . As the limit of zero concentration of mobile ions is approached, simple non-dispersive Debye relaxation behaviour stemming entirely from  $\rho_0$  and  $\varepsilon_{D\infty}$  becomes more and more dominant in the data.

The second curve from the top shows scaled Debye response as a dashed line. Just below it appears the D-material curve after subtraction of electrode effects, exceptionally close indeed to the Debye semicircle here. When the effect of  $\varepsilon_{D\infty}$  is then subtracted, however, the resulting D-material hopping points lie close to the U-model scaled response but show some scatter arising from stringent subtraction effects. Without such subtraction, however, the resulting original modulus formalism approach leads to a  $\beta_1$  estimate of greater than 0.9 instead of 1/3 [6,7,14,19]. Because the C data set involves appreciably smaller electrode effects than does that for the D material, its points after all subtractions lie somewhat closer to the U-model master curve than do the D ones, but their final dispersive hopping responses still show some scatter. Nevertheless, it is clear that both the C and D results scale to the U-model data curve.

Figure 3 presents scaled frequency-response results at the modulus level for the A and B situations. The scaled master curve and the subtracted points lie appreciably above the original data points primarily because of the subtraction of the effects of  $\varepsilon_{D\infty}$  [6,9]. The dispersive B points are poorer, however, than the A ones in the high-frequency region past the peak because electrode

effects dominated the former data more than the latter, resulting in greater subtraction errors. Nevertheless, when the somewhat irregular B data points are fitted to the master curve with CNLS, the resulting open-circle points fit excellently.

Figure 4 shows similar results for the C and D material. Note that even with a magnification factor of 10 the original D data curve is appreciably smaller than the corresponding C one, resulting in greater deviations of the D dispersion points from the master curve than for the C points. Yet again, both Figs. 3 and 4 verify both the scaling approach and the appropriateness of the U fitting model.

In Fig. 5, a traditional log-log scaling plot involving scaled  $\sigma'$  and scaled frequency is presented for all four fits included in Table I. In addition, a curve for a mixed alkali material with two types of mobile ions is included. This curve was scaled to agree with the present master curve at its highest point, and it is evident that it does not agree well with the single-ion U response curve, particularly in the low-frequency region where dispersion is just beginning. The present plots of the scaled data and those in the magnified inset show appreciable electrode-polarization deviations from the master curve at low frequencies for all the data points, but note particularly the deviations appearing at high frequencies for the A data. It is evident that electrode polarization can be important even at high frequencies where it may sometimes be erroneously identified as arising from nearly constant loss processes.

Finally, Fig. 6 shows scaled and fitted results for the dispersive-response parts of the A, B, C, and D data sets. Although, as one would expect, the present scaling is limited only by the accuracy of the estimation of the scaling parameters from the original CNLS fits and is certainly near optimum, it is particularly gratifying that the estimated dispersive data points fit the master curve so well, thus verifying the appropriateness of the U model for these data sets. In the past,

scaling has not usually been attempted for data that involve significant electrode polarization effects, but the present results show that this need not be a limitation, and, as well, it is clear that scaling is unnecessary except to allow comparison of plots for different situations. For most situations, one only need carry out CNLS fits of available data sets to obtain maximum information from them.

#### IV. SUMMARY

The present theoretical analysis shows that the important  $\beta_1$  shape parameter of the K1 dispersive frequency-response model has a unique, constant value of  $1/3$ , and the corresponding high-frequency-limiting log-log slope of  $\sigma'(\nu)$  following from the model is  $2/3$ . These results apply for homogeneous glasses or single crystals with mobile charges of a single type; they therefore are inapplicable to mixed-alkali situations or to mixed electronic and ionic conduction. For single-ion materials, CNLS fits of frequency-response data with  $\beta_1$  taken as a free parameter have led to estimates very close to  $1/3$ . Here it is shown that fixing  $\beta_1$  at  $1/3$ , the U model, leads to excellent fits of data independent of temperature and ion-concentration variation, as expected theoretically and also from an entirely different analysis [28].

Earlier data fittings, not by the author, do not use the K1 model in its corrected modulus form but instead often estimate just the log-log slope (a power-law exponent  $n$ ) of  $\sigma'(\nu)$  at the high-frequency end of the data. Many such estimates are found to be close to  $2/3$ , indicating that electrode polarization effects were negligible at the high-frequency region and thus that the U model might fit the raw data well. In particular, for  $x_c\text{AgI} \cdot (1-x_c)\text{AgPO}_3$   $n$  equalled or was close to  $0.67$  over the concentration range from  $0.2$  to  $0.6$ , and it was  $0.67$  for  $\text{NaPO}_3$  and  $\text{LiPO}_3$  at  $553$

K and 592 K, respectively [32]. Another study [33] yielded  $n = 0.67$  for  $\text{LiPO}_3$  over the range from 295 K to 356 K, suggesting temperature independence over at least the range from 295K to 592 K. Finally, the transition-metal-ion glass,  $0.5\text{P}_2\text{O}_5 \cdot 0.3\text{FeO} \cdot 0.2\text{CaO}$ , identified as a small-polaron hopping conductor, also yielded  $n \cong 0.67$  over the cited range of 290 K to 317 K [34].

Scaling, using the U-model fit results of Table I for variable concentration and temperature, was carried out for  $\rho(\nu)$ ,  $M''(\nu)$ , and  $\sigma'(\nu)$  data and resulted in the complex-plane and frequency-response plots of Figs. 1-6. Scaling was initially unsatisfactory for all these data sets because of the influence of non-dispersive effects associated with electrode polarization and  $\epsilon_{D\infty}$ . When these effects were subtracted to give best estimates of only the dispersive response, however, scaling of the resulting data was successful and led to data points close to those from the exact scaled U model. Fitting of these data points to this model then yielded scaled parameter values in excellent agreement with those of the model. Even when the best available scaling parameters are used, these results suggest that fitting with a model that takes all processes influencing the data into account may be necessary to yield meaningful scaling comparisons, as it certainly is in order to obtain good estimates of hopping parameters from most data.

#### ACKNOWLEDGMENTS

The author is most grateful to all those who provided the data sets used in this study. The insightful comments and suggestions of Dr. J. C. Phillips have been of crucial value.

Table I. Rows A-D:  $\rho(\omega)$ -level U-model CNLS fits to materials with different temperatures and ionic concentrations. The K0 line involves real-part K0 fitting, and MA stands for mixed alkali. All fits used modulus weighting except those of rows A and K0, where proportional weighting was used [18]. Here  $100S_F$  is the percentage value of the relative standard deviation of a fit, and the last column lists its value for fits of the scaled and subtracted data to U-model hopping response..

Type/ Ref.	Material	T (K)	$100S_F$	$10^{-7}\rho_0$ ( $\Omega$ -cm)	$10^7\tau_o$ (s)	$\epsilon_{C1\infty}$	$\epsilon_{D\infty}$	$100\overline{S_F}$ or [ $\beta_0$ ]
U	Scaled master: UM	----	-----	$10^{-7}$	$10^7$	6	0	-----
A/29	0.5Li•0.5La•TiO <sub>3</sub>	179	0.98	6.25	233	25.27	65.01	1.65
B/29	0.5Li•0.5La•TiO <sub>3</sub>	225	0.42	0.018	0.467	17.72	80.13	1.29
C/30	0.2K <sub>2</sub> O•0.8GeO <sub>2</sub>	414	1.13	22.8	87.4	2.60	9.29	1.68
D/30	0.02K <sub>2</sub> O•0.98GeO <sub>2</sub>	602	0.45	24.8	2.82	0.077	9.51	1.99
K0	Fit $\sigma'(\bar{\nu})$ UM data	----	6.6	$9.6 \times 10^{-8}$	$1.8 \times 10^8$	5.94	-----	[0.629]
MA/31	0.3(0.6Na <sub>2</sub> O•0.4Li <sub>2</sub> O) + 0.7B <sub>2</sub> O <sub>3</sub>	Scaled to $\sigma'(\bar{\nu})$ UM data						

## REFERENCES

1. J. C. Phillips, *J. Non-Cryst. Solids* **172-174**, 98 (1994).
2. B. Roling and C. Martiny, *Phys. Rev. Lett.* **85**, 1274 (2000).
3. J. C. Dyre and T. B. Schroder, *Revs. Mod. Phys.* **72**, 873 (2000).
4. W. K. Lee, J. F. Liu, and A. S. Nowick, *Phys. Rev. Lett.* **67**, 1559 (1991).
5. D. L. Sidebottom, *Phys. Rev. Lett.* **82**, 3653 (1999).
6. J. R. Macdonald, *J. Appl. Phys.* **90**, 153 (2001).
7. J. R. Macdonald, *J. Chem. Phys.* **116**, 3401 (2002).
8. J. R. Macdonald, *J. Non-Cryst. Solids* **307-310**, 913 (2002).
9. J. R. Macdonald, *J. Chem. Phys.* **118**, 3258 (2003).
10. *Impedance Spectroscopy – Emphasizing Solid Materials and Systems*, Second edition, edited by E. Barsoukov and J. R. Macdonald (Wiley-Interscience, 2004) to be published.
11. C. P. Lindsay and G. D. Patterson, *J. Chem. Phys.* **73**, 3348 (1980).
12. J. R. Macdonald, *Solid State Ionics* **150**, 263 (2002).
13. H. Scher and M. Lax, *Phys. Rev. B* **7**, 4491 (1973).
14. C. T. Moynihan, L. P. Boesch, and N. L. Laberge, *Phys. Chem. Glasses* **14**, 122 (1973).
15. J. R. Macdonald, *Phys. Rev. B* **63**, 052205 (2001).
16. M. F. Shlesinger and E. W. Montroll, *Proc. Natl. Acad. Sci.* **81**, 1280 (1984).
17. J. Klafter and M. F. Shlesinger, *Proc. Natl. Acad. Sci.* **83**, 848 (1986).
18. J. R. Macdonald and L. D. Potter, Jr., *Solid State Ionics* **23**, 61 (1987); J. R. Macdonald, *J. Computational Phys.* **157**, 280 (2000). The newest WINDOWS version, LEVMW, of the comprehensive LEVM fitting and inversion program may be downloaded at no cost from

<http://www.physics.unc.edu/~macd/>. It includes an extensive manual and executable and full source code. More information about LEVM is provided at this www address.

19. J. R. Macdonald, *J. Appl. Phys.* **95**, 1849 (2004).
20. J. L. Barton, *Verres et Refr.* **20**, 328 (1966).
21. T. Nakajima, *Conference on Electrical Insulation and Dielectric Phenomena* (National Academy of Sciences, Washington, DC), 168-176 (1972).
22. H. Namikawa, *J. Non-Cryst. Solids* **18**, 173 (1975).
23. M. Porto, P. Maass, M. Meyer, A. Bunde, and W. Dieterich, *Phys. Rev. B* **61**, 6057 (2000).
24. J. C. Phillips, *Rep. Prog. Phys.* **59**, 1133 (1996).
25. T. Odagaki and M. Lax, *Phys. Rev. Lett.* **45**, 847 (1980).
26. T. Odagaki and M. Lax, *Phys. Rev. B.* **24**, 5784 (1981).
27. B. Sturman, E. Podivilov, and M. Gorkunov, *Phys. Rev. Lett.* **91**, 176602 (2003).
28. J. R. Macdonald and J. C. Phillips, submitted to *Phys. Rev. Lett.*
29. C. León, J. Santamaria, M. A. Paris, J. Sanz, J. Ibarra, and A. Varez, *J. Non-Cryst. Solids* **235-237**, 753 (1998).
30. H. Jain and S. Krishnaswami, *Solid State Ionics* **105**, 129 (1998).
31. B. Roling and C. Martiny, *Phys. Rev. Lett.* **85**, 1274 (2000).
32. D. L. Sidebottom, *Phys. Rev. B* **61**, 14507 (2000).
33. D. L. Sidebottom, P. F. Green, and R. K. Brow, *Phys. Rev. B* **51**, 2770 (1995).
34. L. Murawski and R. J. Barczynski, *J. Non-Cryst. Solids* **185**, 84 (1995).

## FIGURE CAPTIONS

1. Complex-plane resistivity plots of scaled data for the A and B rows of Table I, before and after subtraction of all non-hopping contributions and including comparison of the latter results with exact U-model hopping response.
2. Stretched complex-plane resistivity plots of scaled data for the C and D rows of Table I, before and after subtraction of all non-hopping contributions and including comparison of the latter results with exact U-model hopping response.
3. Scaled log frequency response of scaled  $M''$  A and B data before and after subtraction of all non-hopping contributions and including comparison of the latter results with exact U-model hopping response. In addition, the open circles show the results of fitting the noisy subtracted B data with the U model.
4. Scaled log frequency response of scaled  $M''$  C and D data before and after subtraction of all non-hopping contributions and including comparison of the latter results with exact U-model hopping response.
5. Log-log scaled frequency response of scaled  $\sigma'$  A and B data before and after subtraction of all non-hopping contributions and including comparison of the latter results with exact U-model hopping response. The solid-circle points are for the mixed alkali data identified in Table I. In addition, the low-frequency part of the response is shown with better resolution in the inset graph.
6. Log-log scaled frequency response of scaled  $\sigma'$  A, B, C, and D data sets fitted to the U-model master curve after subtraction of all non-hopping contributions.

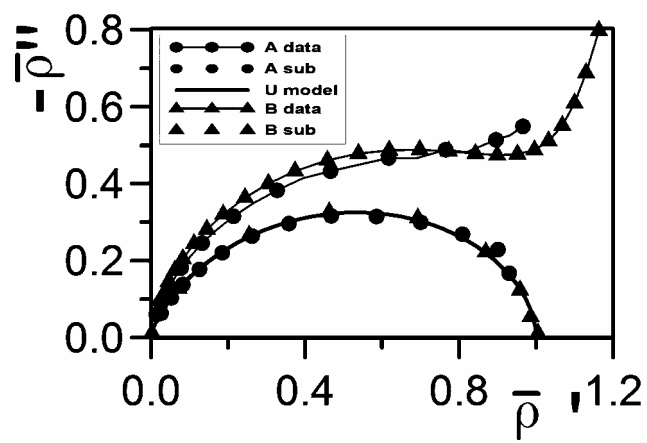


Fig.1

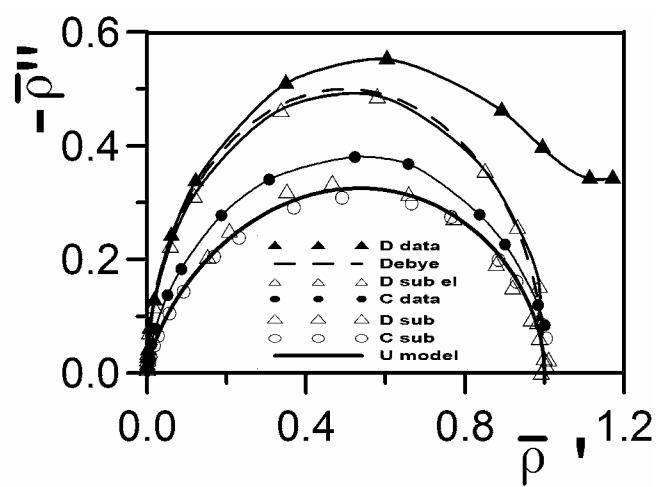


Fig.2

Fig. 3

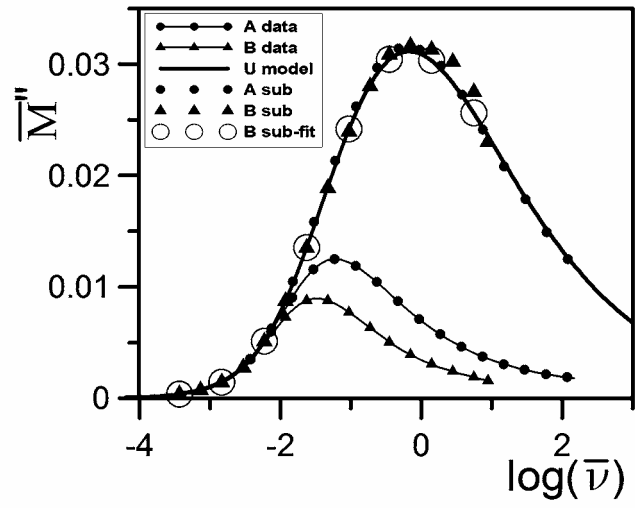


Fig. 4

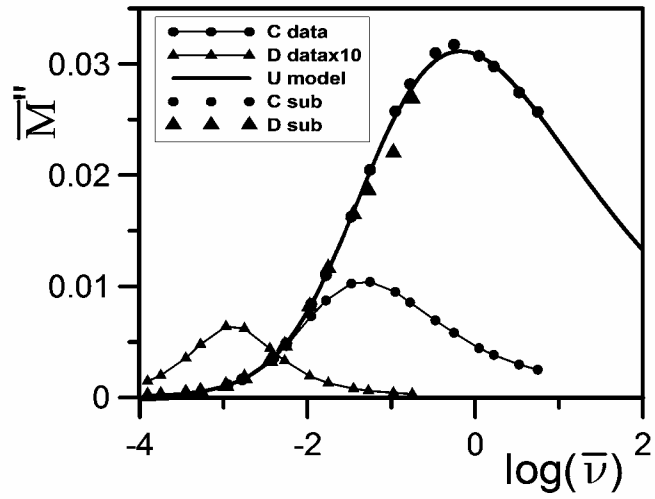


Fig. 5

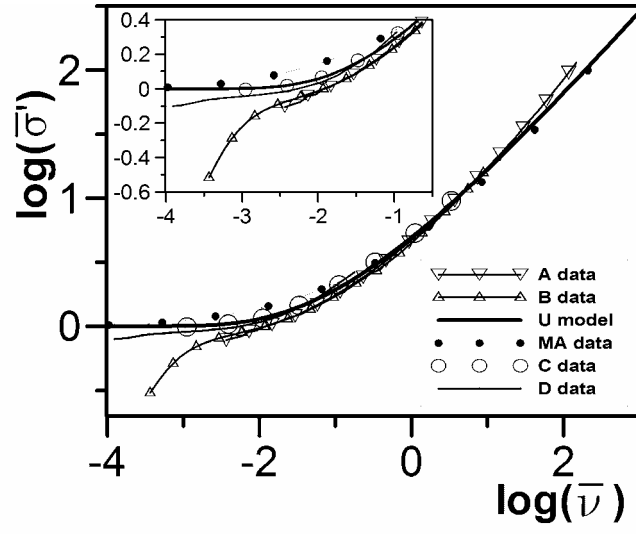


Fig. 6

